Proceedings of the ASME 2010 3rd Joint US-European Fluids Engineering Summer Meeting and 8th International Conference on Nanochannels, Microchannels, and Minichannels
FEDSM-ICNMM2010
August 1-5, 2010, Montreal, Canada

FEDSM-ICNMM2010-30217

MICRO-SCALE FLOW PATTERN CLASSIFICATION BASED ON THE K-MEANS CLUSTERING ALGORITHM.

Sempértegui, Daniel
Escola de Engenharia de São Carlos
University of São Paulo - USP
São Carlos, SP, Brazil
Email: dsempertegui@hotmail.com

Ribastki, Gherhardt
Escola de Engenharia de São Carlos
University of São Paulo - USP
São Carlos, SP, Brazil
Email: ribatski@sc.ups.br

ABTRACT

In the present work, an objective method to characterize two-phase flow pattern was developed and implemented. The method is based on the characteristics of the signals provided by transducers measuring local temperature and pressure plus the intensity of a laser beam crossing the two-phase flow. The statistical characteristics of these signals were used as input features for the k-means clustering method. In order to implement the method, experimental flow patterns were obtained during flow boiling of R245fa in a 2.32 mm ID tube. Experiments were performed for mass velocities from 100 to 700kg/m^{2}s, saturation temperature of 31 ^{o}C and vapor qualities up to 0.99. The cluster classification was compared against flow patterns segregated based on high speed camera images (8000 images/s) and a reasonable agreement was obtained.

NOMENCLATURE

Symbol	Measure	Unit
x	Vapor Quality	-
$h_{L,out}$	Latent Heat	J/kg
P_1 e P_2	Electrical Power 1 e 2	W
G	Mass Velocity	kg/m²s
D	Diameter	mm
$h_{L,in}$	Enthalpy at the inlet	J/kg
$h_{L,out}$	Enthalpy at the outlet	J/kg
T_{sat}	Saturation Temperature	K

INTRODUCTION

In-tube macro-scale two-phase flow pattern transitions and flow characteristics have been targeted by innumerous researchers since the early 40s. These studies were motivated by the fact that heat transfer, pressure drop and the presence of flow instabilities are intrinsically related to the flow configuration and, consequently, the establishment of a good knowledge of the flow characteristics is crucial in order to built reliable heat transfer and pressure drop prediction methods and heat exchanger design tools.

In the late 90s, by the drastic increase in the number of transistors in a microprocessor and its inherent need of dissipating large amounts of energy, a massive number of papers on single-phase and flow boiling in micro-scale channels have started to come up focusing on the development of heat spreaders capable of dissipating heat fluxes up to 3MW/m^2 (see Ribatski et al. [1]). For the same reasons that for macro-scale channel, since the late 90s until now, a significant parcel of studies concerning flow boiling and two-phase flow in micro-scale channels have been performed to characterize flow pattern transitions and two-phase flow characteristics.

Until now, as far as we know, there is no general predictive method for flow pattern transitions in micro-scale channels. Generally, only curve fittings of dimensionless numbers based on restricted databases have been proposed. Additionally, most of these methods are based only on flow pattern visualizations and, so, are affected by the subjective judgments of the observer. Consequently, severe disagreements are observed when these methods are compared.

A tricky aspect in micro-scale two-phase flow and heat transfer studies is how to identify the macro-to-micro scale threshold. A threshold diameter of 3mm was suggested by Kandlikar and Grande [2] for the conventional-to-mini-channel threshold based on the characteristic tube diameters found in distinct applications. In the present work, the same diameter was adopted in order to characterize the macro-to-micro-scale threshold. However, it is important to highlight the fact that such a criterion does not reflect the influence of channel size on physical mechanisms and that a nomenclature based on macro- and micro-scale behaviors (heat transfer, pressure drop and two-phase flow characteristics) is more appropriate than segregate the channels as conventional, mini-meso- and micro-channels based solely on their dimensions.

One of first studies concerning the development of an objective method to identify two-phase flow patterns was performed by Jones and Zuber [3]. Based on the fluctuating signal of X-ray void fraction measurement, they identified air-water flow-patterns in a rectangular channel.

Jones and Zuber [3] have demonstrated that the probability density function (PDF) of the X-ray sign fluctuations can be used as an objective flow pattern discriminator. They have identified the following three flow patterns: bubbly, intermittent (slug + churn) and annular.

An innovative procedure to characterize flow pattern in multi-port micro-scale channels has recently been proposed by Nino et al. [4]. Instead of categorize the flow regime at a given mass flux and quality, they obtained the time fraction in which each flow regime was observed in each channel at a given mass flux and quality. Based on it, flow pattern maps as the one shown in Fig. 1 from Jassim and Newell [5] were built for each experimental condition.

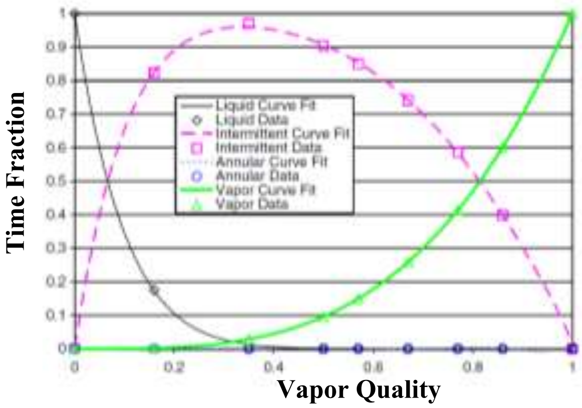

FIGURE 1. PROBABILISTIC FLOW MAP WITH TIME FRACTION CURVE FITS FOR R410A AT 10 ^{O}C AND A MASS FLUX OF 50 kg/m²s IN A 6-PORT MICRO-CHANNEL.

Revellin and Thome [6] conducted experiments for R134a and R245fa evaporating in horizontal 0.509 and 0.709 mm round channels. Based on these data and using an objective approach, Revellin and Thome have segregated the following flow pattern regions: *isolated bubble regime*, characterized by the increase of the bubble frequency with vapor quality; *coalescing bubble regime*, characterized by the decrease of the bubble frequency with vapor quality due to the bubble coalescence process; and *annular flow regime* given by the end of the coalescence process. Then, Revellin and Thome [6] proposed a correlation, according to which the vapor quality for the transition between coalescing bubbles and annular regime is given as a function of the Weber and liquid Reynold numbers, considering all flow liquid.

Based on experimental data for R134a, R245fa and R236fa in a horizontal 1.03 mm round channel and also on the database previously obtained by Revellin and Thome [6], Ong and Thome [7] recently modified the prediction method proposed by Revellin and Thome [6]. They included the effects of saturation pressure on the transition between coalescing bubbles and annular flow regimes introducing a reduced pressure parameter to the previous correlation of Revellin and Thome [6].

Recently, Arcanjo et al. [8] have compared the transition between intermittent flow given by the method of Ong and Thome [7] (coalescing bubbles according to their nomenclature) and the theoretical model by Felcar et al. [9] against their independent experimental data for R134a and R245fa evaporating in a stainless steel tube with diameter of 2.32 mm, mass velocities ranging from 50 to 600 kg/m^2 s and saturation temperatures of 22^{o}C, 31^{o}C and 41^{o}C. Despite the fact that Felcar et al. [9] have developed their model based exclusively on air-water data from the literature, a good agreement was observed by Arcanjo et al. [8] among their data, the model by Felcar et al. [9], and the predictive method by Ong and Thome [7].

Based on the signals of a capacitance sensor, Caniere et al. [10] have built a probabilistic flow pattern map for in-tube air-water horizontal flows. The flow patterns were classified without any subjective visual decisions. The flow regimes were segregated through the c-means clustering algorithm together with a regression technique. The experiments were performed for a 9 mm ID tube. This analysis was based on the average, the variance and a high frequency contribution factor of the capacitance signals. A remarkable agreement was found between a visual classification based on high speed camera images and the probabilistic flow pattern map. In a previous study, Carniere et al. [11] have used the k-means clustering method and similar characteristic signal parameters in order to classify air-water flow patterns in a 9 mm ID tube. The obtained probabilistic flow pattern map presented a good agreement with visual observations and Taitel and Dukler [12] map.

In the present study, two-phase flow patterns in a micro-scale channel were investigated through objective recognition methods. For comparative porpoises, high speed camera images (8000 fps) from the two-phase flows were also obtained. The present analysis was based on electrical signals from the following devices: a micro-thermocouple within the two-phase flow; a micro-piezoelectric pressure transducer having its sensor in contact with the fluid; a laser sensor measuring the intensity of a laser beam crossing a glass tube within the test fluid. The micro-thermocouple and the micro-piezoelectric pressure transducer were located just upstream the test section. First, flow patterns were identified through the Probability Density Function (PDF) and the Power Spectral Density (PSD) applied to these signals. Then, flow pattern probabilistic maps were built through the k-means algorithm method. Good agreement was observed by comparing the probabilistic map and the visual observations.

EXPERIMENTAL DATA

Test apparatus and experimental procedure

The experimental setup is comprised of refrigerant and ethylene-glycol circuits. The refrigerant circuit is schematically shown in Fig. 2. It globally comprises a micropump, to drive the working fluid through the circuit, a pre-heater, to establish the experimental conditions at the inlet of the test section, a test section, a visualization section, a condenser to condense the vapor created in the heated sections, and a reservoir. The water-glycol circuit (not shown) is intended to condense and subcool the fluid in the refrigerant circuit. The cooling effect is obtained by a 60% solution of ethylene glycol/water that operates as intermediate fluid in a system that comprises electrical heaters actuated by PID controllers, 3 water/glycol tanks, heat exchangers and a refrigeration circuit.

In the refrigerant circuit, starting from the subcooler 1, the test fluid flows through the filter to the micropump (self-lubricating without oil). Downstream the micropump, a bypass piping line containing a needle-valve is installed so that together with a frequency controller on the micropump the desired liquid flow rate can be set. There is then a Coriolis mass flow meter and the subcooler 2 to assure that the fluid entering the pre-heater is subcooled. Just upstream the pre-heater inlet, the enthalpy of the liquid is estimated from its temperature T_1 by a 0.25mm thermocouple within the pipe and its pressure p_1 by an absolute pressure transducer. At the pre-heater, the fluid is heated up to the desired condition at the test section inlet. The pre-heater and the test section are horizontal stainless steel tubes 464mm long and 2.32mm ID. Both are heated by applying direct DC current to their surface and are thermally insulated. The power is supplied to them by two independent DC power sources controlled from the data acquisition system. The visualization section is a horizontal fused silica tube with an inner diameter of 2.1mm, a length of 85mm, and is located just downstream to the test section. The two lasers applied to the visualization section are showed Fig. 2 with their respective laser beam detectors. The pre-heater, and the test and visualization sections are connected through junctions made of electrical insulation material and specially designed and machined in such way to match up their ends and keep a smooth and continuous internal surface. Once the fluid leaves the test section its temperature T_2 is determined from a 0.25mm thermocouple within the pipe. The corresponding absolute pressure Δp is estimated from a differential pressure transducer that gives the total pressure drop between the pre-heater inlet and the test section outlet.

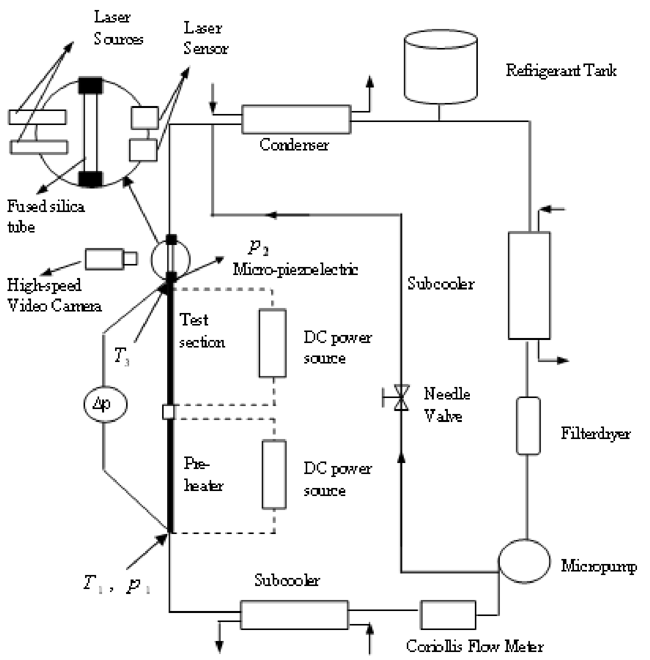

FIGURE 2 – SCHEMATIC DIAGRAM OF THE REFRIGERANT CIRCUIT.

The micro-piezoelectric pressure transducer is installed just upstream the visualization section. It seems that the piezoelectric transducer and the thermocouple are not desestabilizing the flow pattern developed along the heat sections. Then, the working fluid is directed to the tube-in-tube type heat exchanger where it is condensed and subcooled by exchanging heat with the anti freezing ethylene glycol aqueous solution. The refrigerant tank operates as a reservoir of the working fluid and is used to control the saturation pressure in the test section in such way that refrigerant is transferred from the refrigerant circuit to the tank when aiming to reduce the operating pressure. Refrigerant is transferred in the opposite way to increase the operating pressure.

Data reduction

Vapor quality at the inlet of the visualization section. The vapor quality was determined by an energy balance over the pre-heater and the test section according to the Eqn. (1).

$$x = \frac{1}{h_{LG,Out}}\left[\frac{4(P_1+P_2)}{G\pi D^2} + \left(h_{L,in} - h_{L,out}\right)\right] \tag{1}$$

The enthalpy of the liquid at the inlet of the pre-heater, $h_{L,in}$ was estimated based on the measured temperature T_1 and pressure P_1. The liquid enthalpy and the latent heat of vaporization at the visualization section ($h_{L,out}$ and $h_{LG,out}$, respectively) were estimated based on the fluid temperature measured just downstream the visualization section, T_2, and assuming saturated state. In Eqn. (1), P_1 and P_2 are the electrical power supplied by the DC power sources to the heated sections.

Flow patterns. The flow patterns were characterized based on analyses of flow images just at the beginning of the visualization section by high-speed filming. The following flow pattern characterization based on visualizations is applied in the present study:

• Dispersed flow that includes such configurations as bubbly and mist flows, with the gas bubbles in the liquid having smaller diameter than the tube, and gas dispersed in a continuous liquid phase and all the liquid detached from the wall and flowing as small droplets within the gas core;

• Annular flow is characterized by a gas core surrounded by a liquid film on the tube wall;

• Intermittent flow occurs when the flow geometry has a periodic or time varying character;

• Stratified flow (smooth + wavy) is observed when the two phases flow separately with the liquid in the lower region of the tube due to gravitational effects;

So, usual flow pattern denominations found in the literature are included in the four flow patterns abovementioned. Churn, slug, elongated bubbles, plug and pseudo-slug flows are characterized as intermittent flows. Annular and slug-annular are considered as annular flows. Flow pattern images segregated according to the present criteria are illustrated in Fig. 3.

Experimental validation and uncertainties

Compressible volume instabilities also termed in the literature by “explosive boiling” (see Hetsroni et al. [13]) for further details) are a common phenomenon in micro-scale flow boiling. These instabilities can promote severe pressure and temperature oscillations in the flow and seem related to some of discrepancies observed when comparing experimental results from different authors (see Consolini et al. [14]). During the present experimental campaign, such instabilities were not observed and the fluctuations of the fluid temperature and pressure were kept within the uncertainty range of their measurements by acting on a needle valve located upstream the pre-heater.

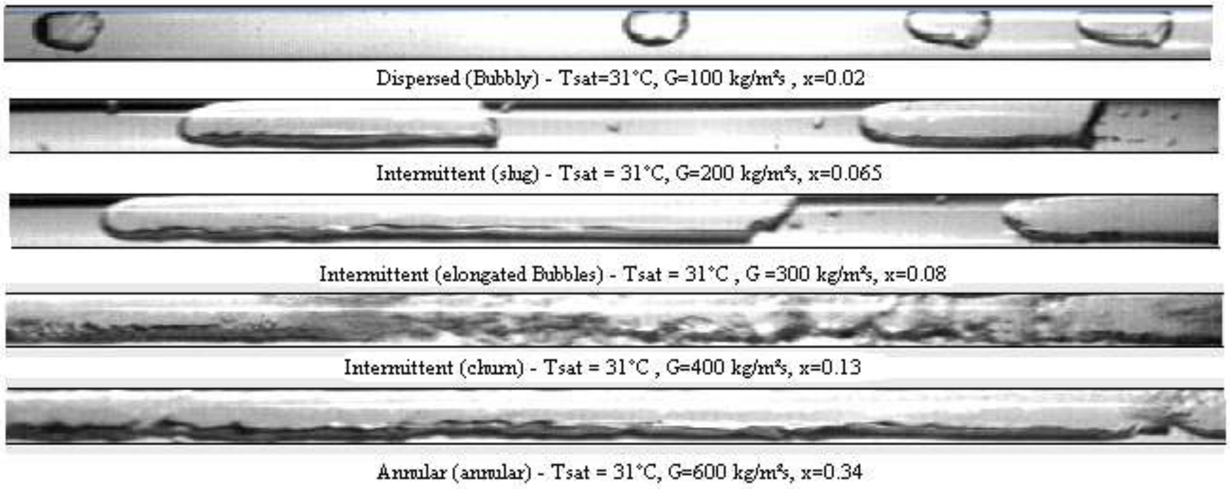

FIGURE 3 – FLOW PATTERNS VISUALIZATIONS AND THEIR NOMENCLATURE, *D=2.32 mm*, R245fa.

Single-phase flow experiments were performed in order to assure the accuracy of the estimated vapor quality and evaluate the effective rate of heat losses during single phase refrigerant, (ΔE/E), defined in the Eqn. (2).

$$\left(\Delta E / E\right) = \frac{\left[\left(\pi D^2/4\right) G \left(h_{out} - h_{in}\right)\right]}{P_1 + P_2} - 1 \qquad (2)$$

Where h_{in} and h_{out} are the refrigerant enthalpies estimated at the pre-heater inlet and just downstream the visualization section, respectively.

As one can see in Fig. 4, the percentage of heat losses is lower than 12% and decreases with increasing the mass velocity.

TABLE 1 – UNCERTAINTY OF MEASURED AND CALCULATED PARAMETERS

Parameter	Uncertainty	Parameter	Uncertainty
D	± 20 μm	Δ*p*	± 0.15 kPa
G	± 0.88%	P_1,P_2	± 0.8%
L	± 1mm	*T*	± 0.15°C
p	± 4.5kPa	*x*	< 5%

Temperature measurements were calibrated and the temperature uncertainty evaluated according to the procedure suggested by Abernethy and Thompson [15]. Accounting for all instrument errors, uncertainties for the calculated parameter were estimated using the method of sequential perturbation according to Moffat [16]. The experimental uncertainties associated with the sensors and calculated parameters are listed in Table 1. ,

K-means Algorithm

The k-means clustering is an unsupervised learning method that consists in the assignment of a set of characteristics into subsets (or clusters) without any help of a supervisor or teacher providing correct answers for each characteristic. In the case of two-phase flow classifications, visual decision is unnecessary. This clustering analysis divides into groups the characteristics, in such a way that certain characteristics on the same cluster are similar in some sense.

The choice of appropriate input features is fundamental to a reasonable performance of the cluster technique. In this work, different input feature combinations were evaluated. The analysis includes statistical characteristics (average, variance, skewness and kurtosis) of the signals of the following devices: the laser beam sensor, the micro-thermocouple and the micro-piezoelectric pressure transducer. Another important factor is the number of clusters necessary to segregate the data in a reasonable way. In the present study, the data were segregated according to three clusters representing the two-phase flow patterns that we initially believe that the algorithm is able to identify.

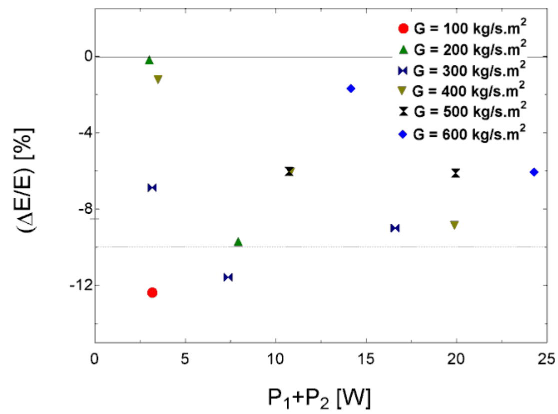

FIGURE 4. EVALUATION OF THE EFFECTIVE RATE OF HEAT TRANSFERRED TO THE SINGLE-PHASE FLOW OF R245fa.

EXPERIMENTAL RESULTS AND DISCUSSIONS

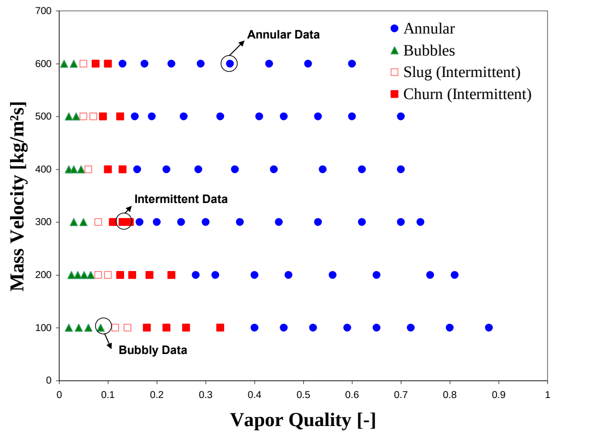

FIGURE 5. FLOW PATTERN DATA FOR R245fa, D = 2.32 mm AND T_{sat} = 31°C

Two-phase flow patterns identification

Figure 5 displays two-phase flow pattern data based on visual observations through a high speed camera. The figure was built based on data for R245fa flowing in a horizontal 2.32 mm ID smooth tube and a saturation temperature of 31°C.

In order to verify if the transducers were able of identifying different flow patterns, one experimental data was selected for each flow regime and the respective electrical signals from the transducers were analyzed. The selected experimental data are indicated in Fig. 5 by their respective symbols within open circles.

In order to verify their capability of identifying two-phase flow patterns, in Fig. 6 to 14 the signal of the pressure, temperature and laser are plotted vs. the time for each data highlighted in Fig. 5. Moreover, the Probability Density Function (PDF) and the Power Espectral Density (PSD) of each signal (Pressure, Temperature and Laser) are also plotted.

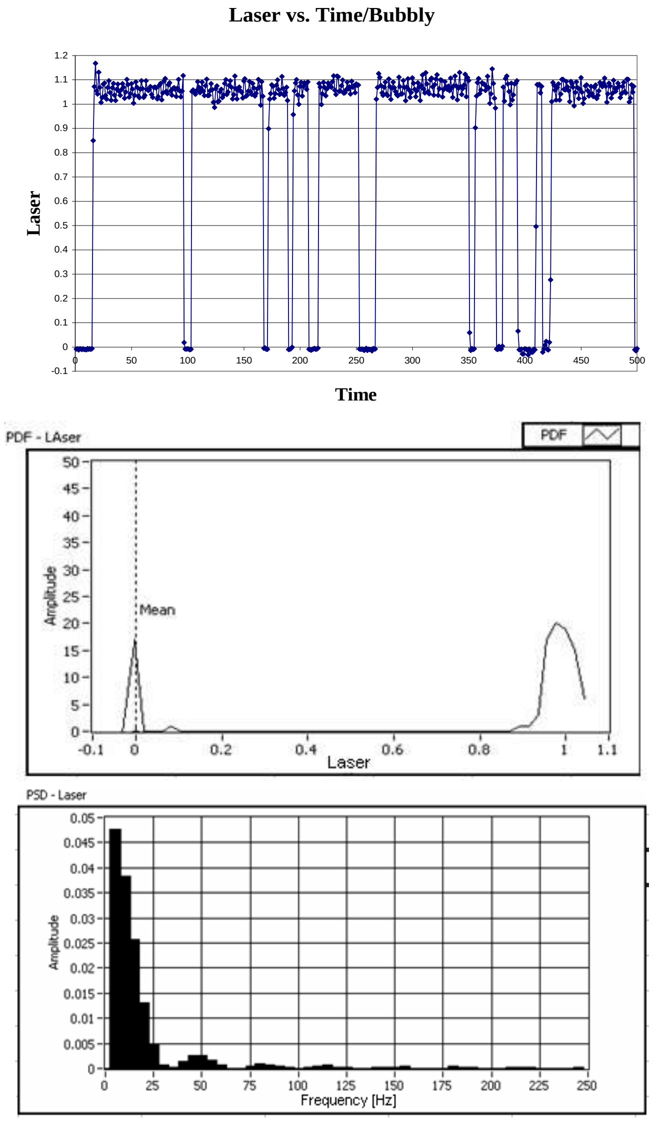

FIGURE 6 – PLOTS DISPLAYING THE CAPTURED SIGNAL VS TIME AND ITS PDF AND PSD FOR THE LASER BEAM. BUBBLY FLOW, R245fa, D = 2.32 mm AND T_{sat} = 31°C, G=100 kg/m²s AND x=0.085

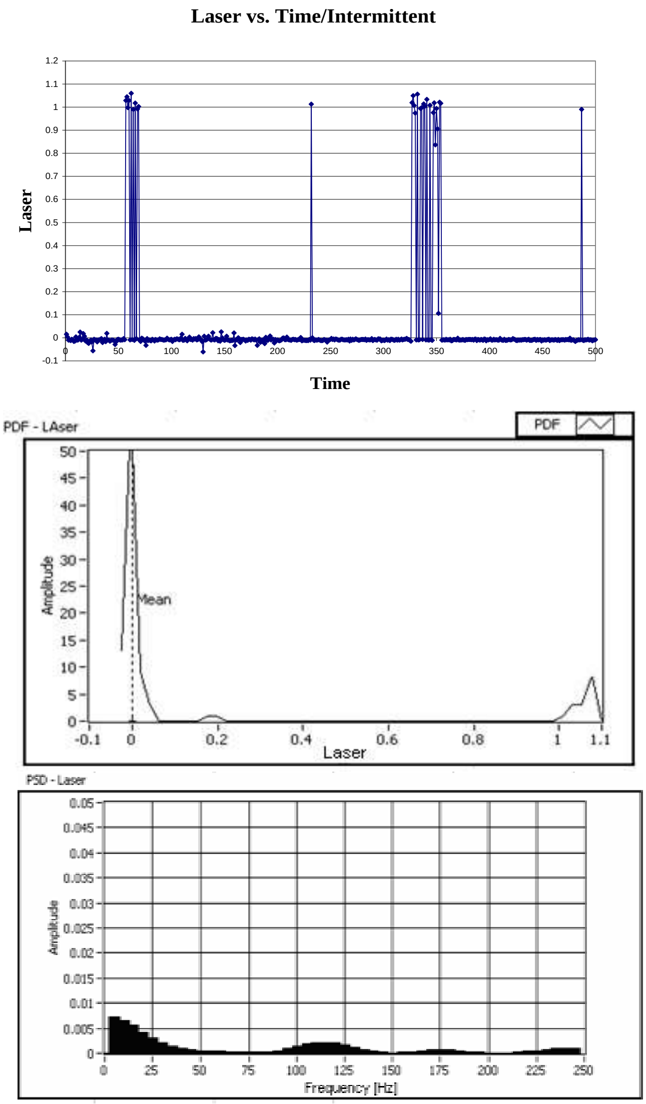

FIGURE 7 – PLOTS DISPLAYING THE CAPTURED SIGNAL VS TIME AND ITS PDF AND PSD FOR THE LASER BEAM. INTERMITTENT FLOW, R245fa D = 2.32 mm ,T_{sat} = 31°C, G=300 kg/m²s AND x=0.13

In Fig. 6, based on data under bubbly flow conditions, the presence of small bubbles is indicated by the attenuation of the laser bean intensity captured by the laser sensor. The attenuation occurs in the presence of vapor bubbles due to the laser reflection and divergence in the presence of liquid-vapor interfaces. The Probability Density Function (PDF) of this signal presents two peaks which are related to the occurrence of liquid and vapor plugs. The PSD plot shows a peak at low frequencies that corresponds to the bubble frequency. By counting the number of bubbles per second from the high speed films, it was found an average bubble frequency of 9 bubbles/s. This value matches the peak in the PDF plot.

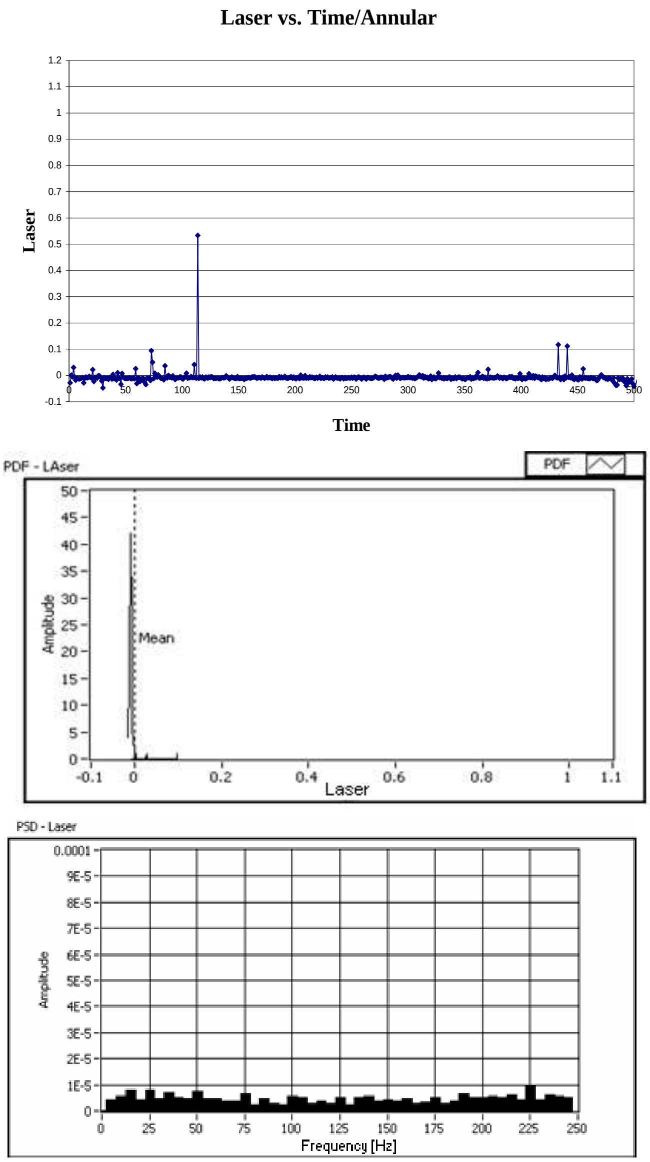

FIGURE 8 – PLOTS DISPLAYING THE CAPTURED SIGNAL VS TIME AND ITS PDF AND PSD FOR THE LASER BEAM. ANNULAR FLOW, R245fa, D = 2.32 mm T_{sat} = 31°C, G=600 kg/m²s AND x=0.34

Figure 7 displays a similar analysis for intermittent flow. It is inferred the presence of elongated bubbles, corresponding to the region of the minimum values in the plot, intercalated by liquid slugs, corresponding to the regions displaying the maximum values in the plot. As for bubbly flow, the PDF plot shows two peaks corresponding in the presenting case to elongated bubbles and the liquid slugs. However, while in case of bubbly flow the two peaks presents almost the same amplitude, in case of intermittent flows the amplitude of the peak corresponding to the presence of elongated bubbles is much higher. The PSD plot presents again a peak at low frequencies which, based on the time delay between two liquid slugs, seems to correspond to the elongated bubble frequency.

For annular flow, the analysis was performed for a mass velocity of 600 kg/m²s and a vapor quality of 0.34. Figure 8 displays the results for annular flow. According to this figure, the laser beam signal presents an almost constant value around 0 and some unexpected changes. Once we have changed from intermittent to annular flows the PDF started to have just one peak at the minimum value of the laser and the PSD does not present any peaks.

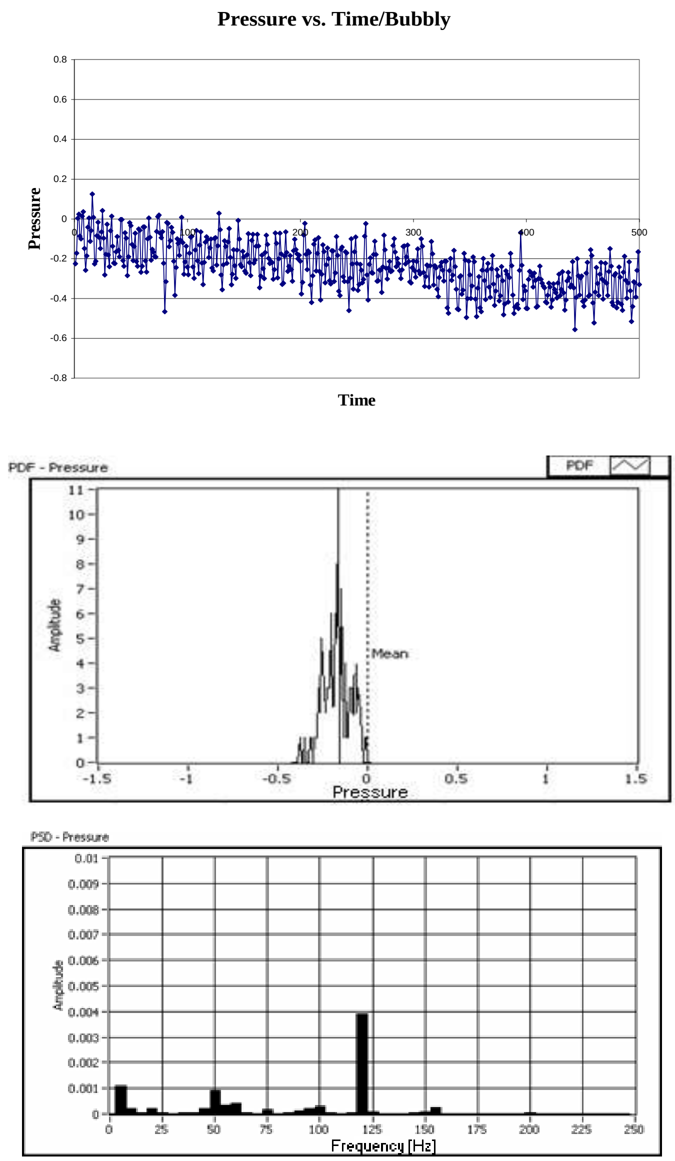

FIGURE 9. PLOTS DISPLAYING THE CAPTURED SIGNAL VS TIME AND ITS PDF AND PSD FOR THE PRESSURE TRANSDUCER. BUBBLY FLOW, R245FA, D = 2.32 mm, T_{sat} = 31°C, G=100 kg/m²s AND x=0.085

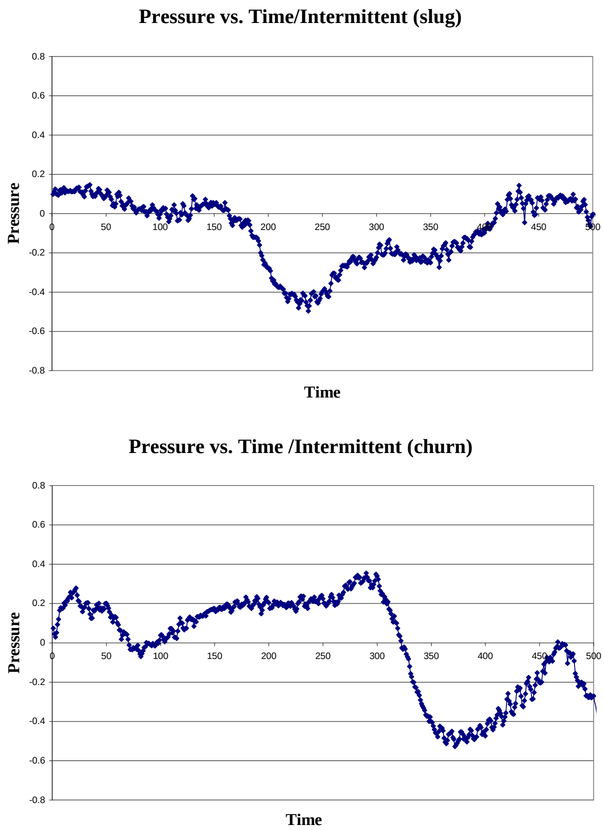

FIGURE 10. COMPARISON BETWEEN THE CAPTURED SIGNAL VS TIME FOR SLUG AND CHURN FLOWS R245fa, D = 2.32 mn AND T_{sat} = 31°C

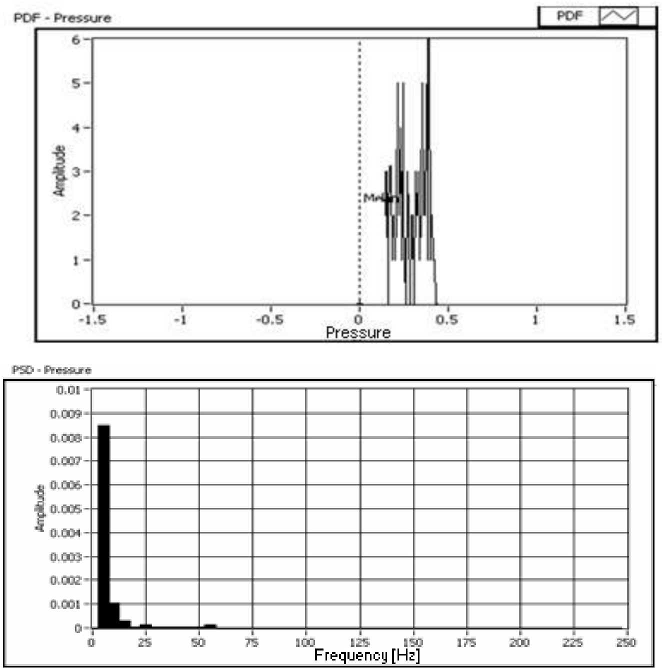

FIGURE 11. PDF AND PSD OF THE PRESSURE SIGNAL FOR INTERMITTENT FLOW (SLUG), R245fa, D = 2.32 MM AND T_{sat} = 31°c, G=300 kg/m²s AND x=0.13

An analysis of the signal from the piezoelectric transducer is displayed in Figs. 9 to 12. By comparing the plots showing the pressure signal vs. time displayed in Figs. 9, 10 and 12, a difference among the flow patterns through comparisons of the transducer signal can be easily recognized. In case of bubbly flow, the pressure signal oscillates with a much higher frequency than for intermittent and annular flows. This frequency is around to 125 Hz according to the PDF analysis shown in Fig. 9. So, much higher than the bubbly frequency that was found equal to 9 bubbles/s. It was already expected that the combination of forces acting on the bubbles would not affect the local pressure measured by the pressure transducer since the bubbles are smaller than the tube diameter. In the case of elongated bubbles, it seems that the passages of elongated bubbles are detected by the sensor as shown in Fig. 10.

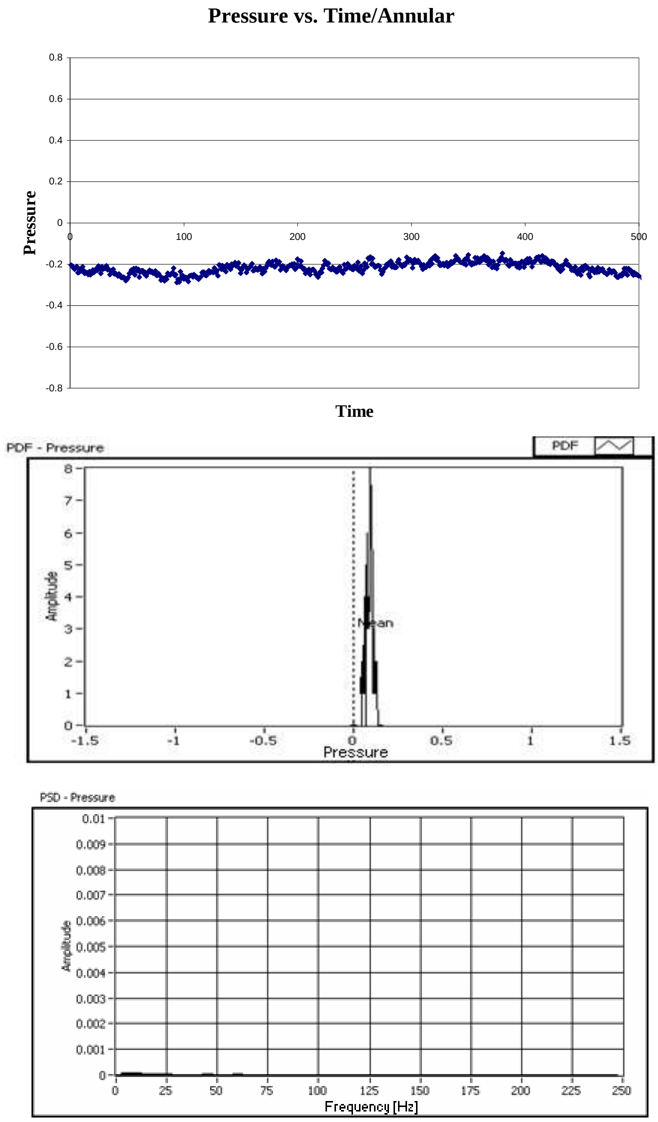

FIGURE 12 –PLOTS DISPLAYING THE CAPTURED SIGNAL VS TIME AND ITS PDF AND PSD FOR THE PRESSURE TRANSDUCER. ANNULAR FLOW, R245fa, D = 2.32 mm AND T_{sat} = 31°C, G=600 kg/m²s AND x=0.34

In case of churn flow a similar behavior was detected. The peak in the PSD plot shown in Fig. 11, for which the experimental conditions correspond to the slug flow in Fig.

10, coincides with the elongated bubble frequency. The PSD plots for the annular flow data are shown in Fig. 12. As previously expected there is no oscillations in the pressure signal, since the forces acting in the sensor due to the two-phase flow topography are almost constants. Consequently, a peak in the PSD plot is not displayed for annular flow. By comparing Figs. 9, 11 and 12, it is concluded that he PDF analysis of the pressure signal does not provide any relevant information about the two-phase flow configuration.

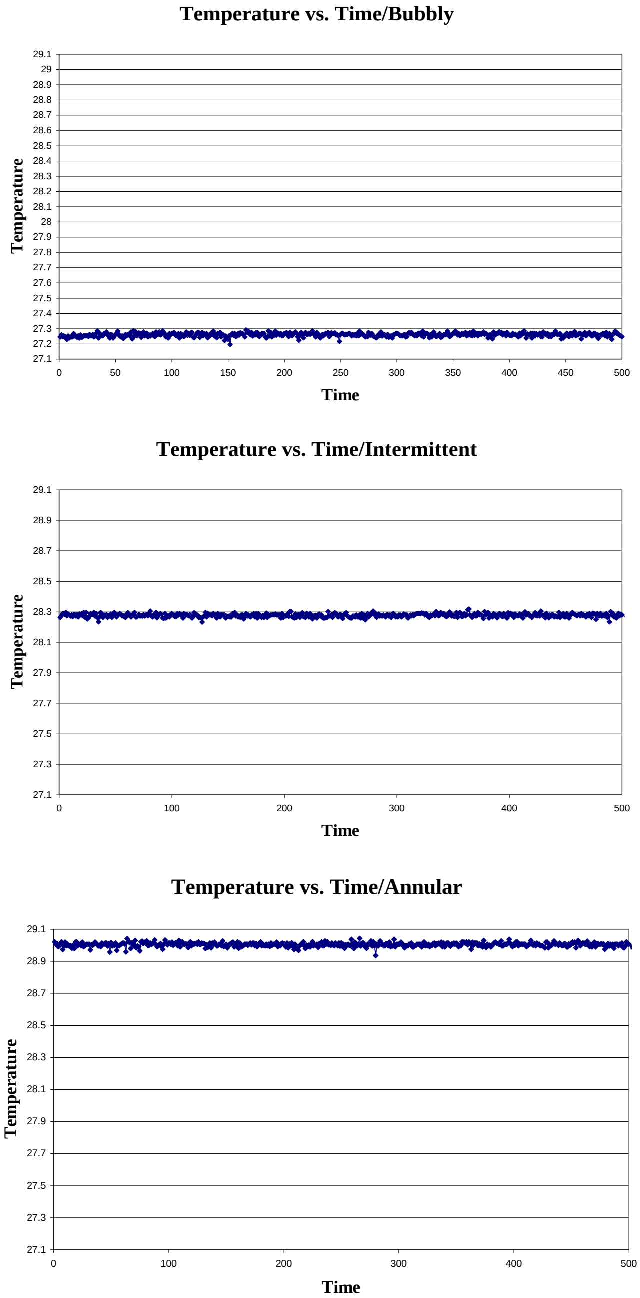

FIGURE 13 – FLUID TEMPERATURE VARIATION WITH TIME: (A) BUBBLY FLOW, (B) INTERMITTENT FLOW; (C) ANNULAR FLOW. R245fa, D = 2.32 mm AND T_{sat} = 31°C.

Figure 13 illustrates the variation of the local fluid temperature with time. According to this figure, the temperature is almost constant with the time and its variation is within the range of uncertainty of its measurements. Such a result highlighted the fact that the experiments were performed almost under the absence of thermal-instabilities which, as aforementioned, can cause temperature variations up to 10^{o}C according to a frequency from 2 to 10 Hz

To investigate the reasons for an almost constant fluid temperature, the thermocouple response-time was roughly estimated and a value of 0.3s was found to indicate a variation just above the uncertainty of the temperature measurements. So, the thermocouple is unable of capturing small fluctuations in the liquid temperature and the adoption of thermocouple wires having smaller diameters and hot junctions are recommended for further studies.

Two-phase flow pattern map

Based on the previous analysis, the signals from the laser bean sensor and the piezoelectric pressure transducer were considered for identifying the flow patterns through the k-means algorithm. The average, the variance, the skewness and the kurtosis of each signal were calculated. Best flow pattern recognition results were found when using the following input features: the average of the laser attenuation signal (Avg_L), the variance of the laser attenuation signal (Var_L), the average of the pressure signal (Avg_P) and the variance of the pressure signal (Var_P).

For the selected input features, all the possible combinations of three of them were evaluated according to the k-means clustering algorithm. In general the best clustering results were obtained by using the following input variables: Avg_L, Var_L and Var_P with all weight parameters set to one. This input matrix was used to determine the clusters and generate the two-phase flow pattern map. The k-means clustering method was applied to generate two-phase flow pattern map with 3 and 4 cluster centers. The two-phase flow map generated for 3-cluster centers is shown in the Fig. 14. In this figure, the lines represent the boundaries of the 3 clusters and the symbols the flow patterns characterized from the analyses of the flow images. In Fig. 14, for the transitions between intermittent (slug + churn) to annular and bubbly to intermittent (slug + churn), reasonable agreements are displayed between both characterization methods.

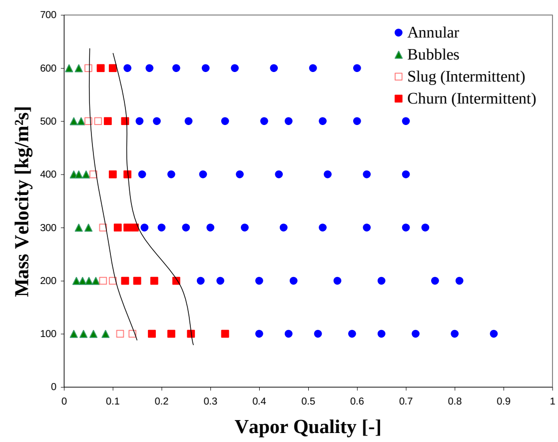

FIGURE 14. COMPARISON BETWEEN THE PROBABILISTIC TWO-PHASE FLOW PATTERN MAP WITH 3-CLUSTERS (LINES) AND THE VISUAL OBSERVATIONS (SYMBOLS) FOR R245fa, D = 2.32 mm ,T_{sat} = 31°C

A comparison between the probabilistic two-phase flow pattern map containing 4-cluster centers and the visualizations is shown in Fig. 15. This new map is basically similar to the previous one. The only difference is that one additional group for low vapor quality and mass velocity is identified which is characterized by much smaller bubbly frequencies during bubbly flow.

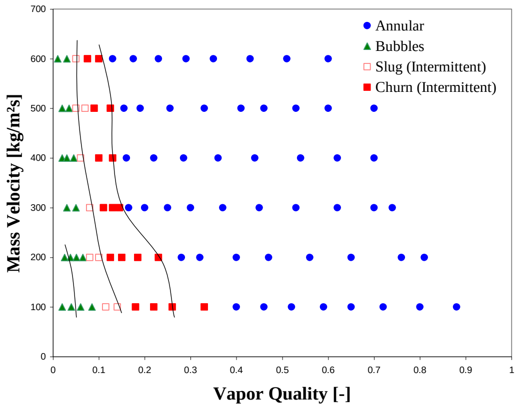

FIGURE 15. COMPARISON BETWEEN THE PROBABILISTIC TWO-PHASE FLOW PATTERN MAP WITH 4-CLUSTERS (LINES) AND THE VISUAL OBSERVATIONS (SYMBOLS) FOR R245FA, D = 2.32 mm T_{sat} = 31°C

CONCLUSIONS

A summary of the conclusions drawn from the results and analysis of the present experimental investigation on flow pattern based on k-means clustering is as follows:

a) Laser beam signal identified reasonably well the two-phase flow patterns;
b) It is possible to characterize the flow patterns from the analysis of the pressure signal;
c) The flow pattern characterization from the analysis of the transient fluid temperature did not work. However, it is speculated that good results can be achieved by using thermocouple wires having smaller diameters and hot junctions, due to its faster response-time;
d) The two-phase flow map created based on a k-means clustering analysis has presents good agreement with visual observations;

ACKNOWLEDGMENTS

The authors gratefully acknowledge the financial support under contract numbers 2005/60031-0, 2006/52089-1 and 2008/56930-8 given by FAPESP (The State of São Paulo Research Foundation, Brazil). The technical support given to this investigation by Mr. José Roberto Bogni is also appreciated and deeply recognized.

REFERENCES

[1] Ribatski, G., Cabezas-Gómez, L., Navarro, H.A., and Saiz-Jabardo, J.M., 2009, "The Advantages of Evaporation in Micro-Scale channels to Cool Microeletronic Devices", Reterm-Thermal Engineering, Vol. 6, pp. 34–39.

[2] Kandlikar, S.G., Grande, W.J., 2003, "Evolution of microchannel flow passages - Thermohydraulic performance and fabrication technology", Heat Transfer Eng., Vol. 24, pp. 3-17.

[3] Jones, O., and Zuber, N., 1975, "The Interrelation Between Void Fraction Fluctuations and Flow Patterns in Two-Phase Flow", Int. J. Multiphase Flow, Vol. 2, pp. 273-306.

[4] Nino, V., Hrnjak, P., and Newell T., 2003, "Two-Phase Flow Visualization of R134A in a Multiport Microchannel Tube", Heat Transfer Eng., Vol. 24, pp. 41–52.

[5] Jassim, E., and Newell, T., 2006., "Prediction of Two-Phase Pressure Drop and Void Fraction in Microchannels Using Probabilistic Flow Regime Mapping", Int. J. Heat Mass Transfer, Vol 49, pp. 2446–2457.

[6] Revellin, R., and Thome, J.R., 2007, "A New Type of Diabatic Flow Pattern Map for Boiling Heat Transfer in Microchannels", J. Micromech. Microeng., Vol. 17, pp. 788–796.

[7] Ong, C.L., and Thome, J.R., 2009, "Flow Boiling Heat Transfer of R134a, R236fa and R245fa in a Horizontal 1.030 mm. Circular Channel", Exp. Therm. Fluid Sci., Vol. 33, pp. 651-663.

[8] Arcanjo, A.A., Freitas, J.O., Tibiriçá, C.B., and Ribatski, G., 2010, "Evaluation of Flow Patterns and Elongated Bubble Characteristics During the Flow Boiling of Halocarbon Refrigerants in a Micro-Scale Channel", Exp. Thermal and Fluid Sci., Vol. 34, pp. 766-775.

[9] Felcar, H.O.M., Ribatski, G., and Saiz-Jabardo, J.M., 2007, "A Gas Liquid Flow Pattern Predictive Method for Macro- and Mini-Scale Round Channels", Proc. 10th UK Heat Transfer Conference, Edinburgh, Scotland.

[10] Canière, H., Bauwens, B., T'Joen, C., and De Paepe, M., 2009, "Probabilistic Mapping of Adiabatic Horizontal Two-phase Flow by Capacitance Signal Feature Clustering ", Int. J. Multiphase Flow, Vol. 35, pp. 650-660.

[11] Canière, H., Bauwens, B., T'Joen, C., Boullart, L., and De Paepe, M., 2008, "Towards Objective Flow Pattern Mapping with the K-means Clustering ", 6th Int. Conf. on Heat Transfer, Fluid Mechanics and Thermodynamics, Pretoria, South Africa.

[12] Taitel, Y., and Dukler, A.E., 1976, "A Model for Predicting Regime Transitions in Horizontal and Near Horizontal Gas-Liquid Flow", AIChE Journal, Vol. 22, pp. 47-55.

[13] Hetsroni, G., Mosyak, A., Pogrebnyak, E., and Segal Z., 2005, "Explosive boiling of water in parallel micro-channels", *Int. J. Multiphase Flow*, Vol. 31, pp. 371-392.

[14] Consolini, L., Ribatski, G., Wei, Z., Xu, J., and Thome, J.R., 2007, "Heat Transfer in Confined Forced Flow-Boiling", *Heat Transfer Engineering*, Vol. 28, pp. 826-833.

[15] Abernethy, R.B., and Thompson, J.W., 1973, "Handbook Uncertainty in Gas Turbine Measurements", Arnold *Engineering Development Center*, Arnold Air Force Station, Tennessee.

[16] Moffat, R.J., 1988, "Describing the Uncertainties in Experimental Results", Exp. Thermal Fluid Sci., Vol. 1, pp. 3-17.